Nanoscale

Accepted Manuscript

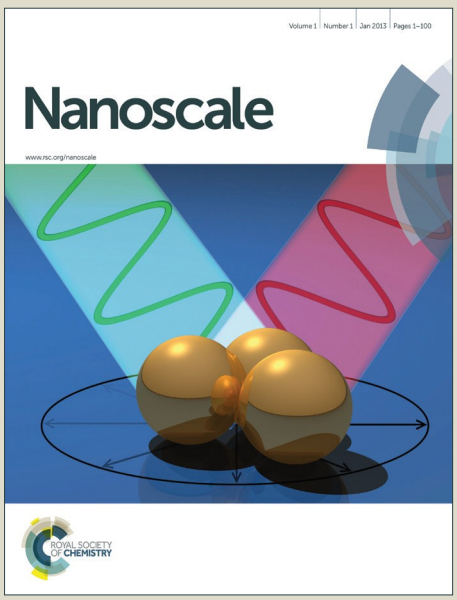

ROYAL SOCIETY OF CHEMISTRY

www.rsc.org/nanoscale

Nanoscale

RSCPublishing

ARTICLE

A nanoglass alloying immiscible Fe and Cu at the nanoscale

Cite this: DOI: 10.1039/x0xx00000x

Na Chen,[a,b,c*] Di Wang,[a] Tao Feng,[a] Robert Kruk,[a] Ke-fu Yao,[c] Dmtri V. Louzguine-Luzgin,[b] Horst Hahn[a,d,e] and Herbert Gleiter[a,d],

Received 00th ,
Accepted 00th

DOI: 10.1039/x0xx00000x

www.rsc.org/

Synthesized from ultrafine particles with a bottom-up approach, nanoglasses are of particular importance in pursuing unique properties. Here, we design a metallic nanoglass alloy from two components of ~$Cu_{64}Sc_{36}$ and ~$Fe_{90}Sc_{10}$ nanoglasses. With nanoalloying mutually immiscible Fe and Cu, the properties of the nanoglass alloys can be tuned by varying the proportions of the ~$Fe_{90}Sc_{10}$ component. This offers opportunity to create novel metallic glass nanocomposites and sheds light on building a structure-property correlation for the nanoglass alloys.

Introduction

Metallic nanoglasses (MNGs) or nanostructured metallic glasses are created by inert gas condensation, sputter deposition or nanomoulding with metallic glasses.[1-7] With unique nanogranular structures, the MNGs show very promising properties, such as highly catalytic activity, excellent biocompatibility or room temperature ferromagnetism superior to their nanodomain-free metallic glass counterparts.[1-6, 8, 9] Basically the volume fraction of atoms located at the glass-glass interfaces increases with reducing the granule size, which plays an important role in determining the performance of these MNGs. Similar to nanocrystalline materials, varying the granule size of the MNGs thereby modifies their properties.[10] This may offer an effective way to improve the extremely low tensile ductility of bulk metallic glasses (BMGs), which is considered a bottleneck to hinder their widespread applications.[4, 10-12] In addition, the inert gas condensation, as one of the representative approaches for producing nanoglasses, enables a mixture of immiscible elements in the solid states.[13]

Alloys with immiscible elements are of both scientific and technological importance due to the potential creation of new structures for tuning the properties.[14-16] Exploring the existing non-equilibrium processes such as vapour deposition, liquid quenching or mechanical alloying, alloying immiscible elements has been realized in a number of systems including Ag-Cu, Pt-Au and Co-Cu alloys.[17-19] In particular, formation of amorphous alloys from these immiscible systems has raised tremendous interest ascribed to their significance in understanding the glass nature and the drastic property change from the crystalline counterparts. Usually introducing immiscible elements to the glass-forming alloy systems promotes nanoscale phase separation and enhances the global plasticity of BMGs.[20-22] To date, most of the MNGs are formed from one alloy, in which the nanoglass cores and the glass-glass interfaces share the same composition.[1-6] This raises a concern about the possibility to create a MNG alloy from two nanoglasses with immiscible elements. The $Fe_{90}Sc_{10}$ alloy is recognized to be a model nanoglass system with room-temperature ferromagnetism.[5, 6] To achieve the above target, we need to develop a new nanoglass system that contains at least one element mutually immiscible with Fe in the $Fe_{90}Sc_{10}$ nanoglass. Owing to a positive heat of mixing (ΔH=13 kJ/mol) between Fe and Cu, a binary Cu-Sc system is selected and proves to be a nanoglass former. Accordingly, the MNG alloys are created from the two nanoglass components of ~$Cu_{64}Sc_{36}$ and ~$Fe_{90}Sc_{10}$. Furthermore, the ferromagnetism of the MNG alloys can be tuned by varying the proportions of one nanoglass component.

Results and discussion

The experimental setup for formation of the MNG alloys from two nanoglasses is illustrated in Fig. 1a and b, respectively. Nanometer-sized particles evaporate from the independent ingots of Fe-Sc and Cu-Sc alloys (Figure 1(a) and (b)). By rotating the cold finger, the nanometer-sized glassy particles with different chemical compositions are collected and mixed. A transmission electron microscopy (TEM) is applied to confirm the glassy nature of the condensated particles, which are directly deposited onto the gold grid coated with holey amorphous carbon film and additional complete 2 nm thin carbon films. The very thin 2 nm-film support beneath the nanoparticles enables clear imaging with little interference from the contrast of support. As shown in Figure 1(c),

the particles have an average size of about 10 nm. The selected area electron diffraction (SAED) pattern (Figure 1(c) insert) consists of two broad diffraction haloes without sharp diffraction rings or spots resulted from crystalline phases. This indicates that these nanometer-sized particles are mostly glassy. A high resolution (HR)TEM image shows one individual particle and several particles in contact with each other. All of them have maze-like patterns in the projected view, typical for glassy structures (Figure 1(d)). In some regions few crystallized nanoparticles are also observed, which can be indexed to be Sc_2O_3 (not shown here).

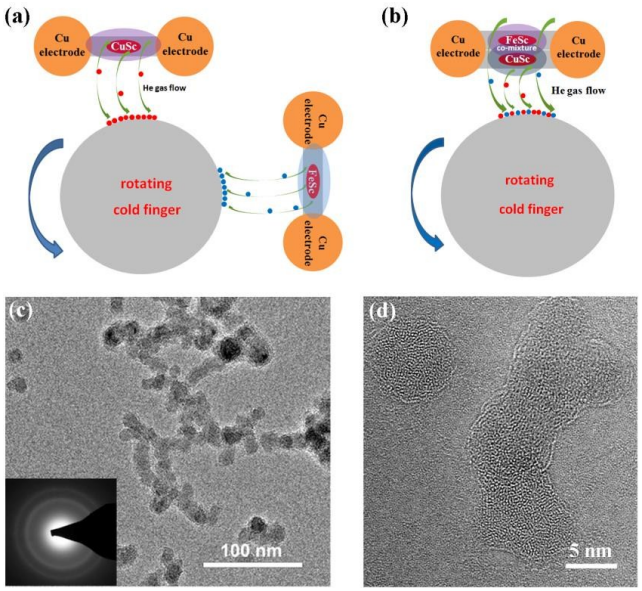

Figure 1 Schematic diagrams for formation of a MNG alloy from two ingots in the tungsten boats (a) located in two pairs of Cu electrodes and (b) located in one pair of Cu electrodes; (c) The TEM image of the MNG alloy powders. The inset is the selected area electron diffraction (SAED) pattern, revealing the sample's glassy nature and (d) the HRTEM image showing formation of one glassy particle and several glassy particles contacting with each other.

The mixed MNG powders shown in Figure 1(c) are subsequently collected in a small holder and subjected to an external pressure of 1.5 GPa under a high vacuum condition of around 10^{-6} Pa. Using the experimental setup shown in Figure 1(a), the compacted cylindrical sample of the MNG-1 alloy with a diameter of 8 mm displays a shiny surface as shown in the inset at the bottom of Figure 2(a). The SAED pattern in the inset of Figure 2(a) is similar to that obtained for the mixed MNG alloy powders (Figure 1(c)). The HRTEM image of the MNG-1 alloy exhibits typical glassy structures with clear contrasts, indicative of its inhomogeneous structure. The dark-field scanning transmission electron microscopy (DF-STEM) image displays a nanogranular structure as observed in Figure 2(b). The compositional mapping derived from the STEM-EDS spectrum imaging, reveals Cu-rich and Fe-rich regions separated from each other (see Figure 2(c)-(f)). Using the installed multivariate data analysis software equipped with a method of multivariate curve resolution (MCR), the compositions of the two components Cu-Sc and Fe-Sc nanoglasses can be determined to be ~$Cu_{64}Sc_{36}$ and ~$Fe_{90}Sc_{10}$, respectively. MCR is defined as a group of techniques which help resolve multicomponent systems or mixtures by determining the variable number, their response profiles and their estimated concentrations.[23, 24] This method is mainly based on a bilinear model, which allows the decomposition of the raw data matrix into the product of two data matrices. Each of them includes the pure response profiles of the n components associated with the row and the column direction of the initial data matrix, respectively. The detailed information for this technique can be found in Refs 23 and 24.

From the above structural characterization one can conclude that two nanoglasses of ~$Cu_{64}Sc_{36}$ and ~$Fe_{90}Sc_{10}$ coexist in one alloy and show clear boundaries between them due to the chemically immiscible nature of Cu and Fe. The structural inhomogeneity reaches several hundred nanometers because the aggregation of the nanoglass particles from the individual nanoglass component occurs before they intermix with each other on the cold finger. To avoid formation of such big clusters, we design an alternative experimental setup as shown in Figure 1(b) to alloy the immiscible Fe and Cu at the nanoscale.

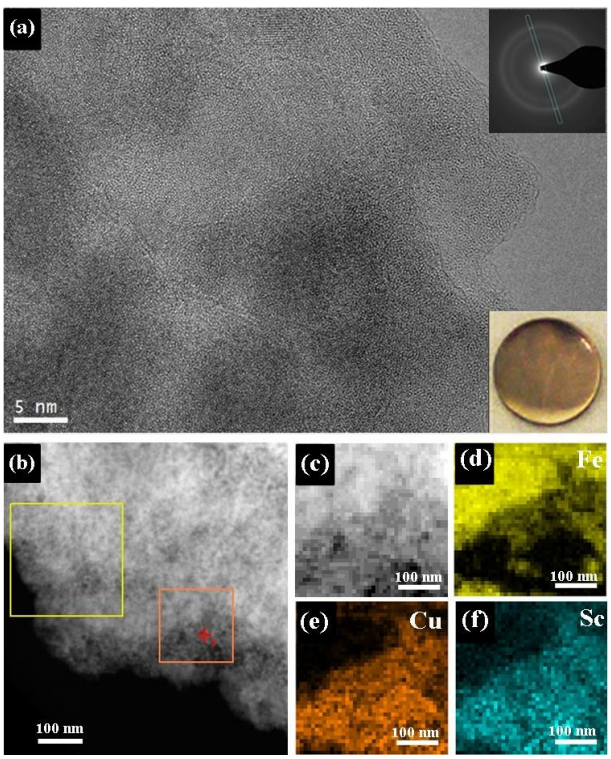

Figure 2 (a) The HRTEM of the bulk MNG-1 alloy with a diamter of 8 mm. The inset are the SAED pattern and the image of the bulk sample; (b) and (c) The STEM images; (d)-(f) The corresponding compositional mappings of Fe, Cu and Sc, respectively.

As shown in Figure 3(a), the produced bulk MNG-2 alloy shows a typical maze-like pattern without obvious contrast, indicative of a relatively homogeneous glassy structure. The fast Fourier transform (FFT) pattern shows two diffuse haloes (Inset of Figure 3(a)), similar to the SAED pattern shown in Figure 3(b). This further verifies that the two nanoglasses still exist and are intermixed at the nanoscale in the MNG-2 alloy. In addition, the granular structure observed in the MNG-1 alloy is absent in the MNG-2 alloy (Figure 2(b) and 3(b)). The detailed compositional mapping reveals relatively homogeneous distributions of Cu, Fe and Sc compared to those of the MNG-1 alloy (Figure 3(d)-(f)). To confirm that there is indeed no compositional segregation as large as that observed in the MNG-1 alloy, we conducted STEM-EDX mapping at different areas and similar results were observed as shown in Supplementary Figure 1. Nanoalloying of immiscible Fe and Cu is therefore obtained in the MNG-2 alloy.

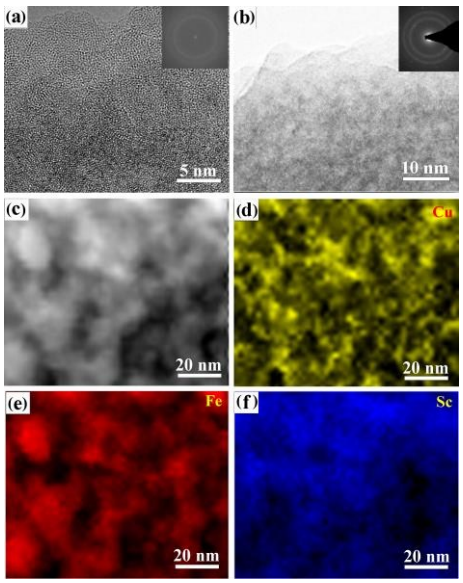

Figure 3 (a) The HRTEM of the bulk MNG-2 alloy with a diamter of 8 mm; (b) The bright field (BF)-TEM image; (c) The STEM image and (d)-(f) the corresponding compositional mappings of Cu, Fe and Sc, respectively.

The $Fe_{90}Sc_{10}$ MNG has shown room-temperature ferromagnetism whereas the rapid solidified $Fe_{90}Sc_{10}$ MG ribbons are paramagnetic.[6] Similar to the MG ribbons, the isolated $Fe_{90}Sc_{10}$ nanoglass particles are paramagnetic. A further structural study of the $Fe_{90}Sc_{10}$ MNG shows that the interfaces present a wider interatomic spacing of Fe-Fe atomic pairs arising from a lower atomic density than that of the nanoglass cores.[5, 6, 25] The magnetic moment is expected to monotonically increase with the lattice constant.[26, 27] Together these studies provide compelling evidence that the ferromagnetism primarily stems from the interfaces. Accordingly, one can expect to modify the magnetic properties by varying the amount of the interfaces in the MNGs. To achieve this, we produced different MNG-2 alloys by controlling the percentage of the $Fe_{90}Sc_{10}$ MNG. Increasing the $Fe_{90}Sc_{10}$ component from 23 at.% to 74 at.%, the magnetization increases from 0.63 μ_B per Fe atom to 1.12 μ_B per Fe atom if subjected to an external field of 20 kOe (Figure 4(a)). The introduction of the ~$Cu_{64}Sc_{36}$ nanoglass component reduces the opportunity for the ~$Fe_{90}Sc_{10}$ nanoparticles to contact with each other, thereby leading to a reduction in the amount of the interfaces between the $Fe_{90}Sc_{10}$ nanoparticles. This further confirms that the effect of the interfaces on the ferromagnetism prevails over the nanoglass cores. As shown in Figure 4(a), the magnetization of the $(Fe_{90}Sc_{10})_{0.74}(Cu_{64}Sc_{36})_{0.26}$ MNG-2 alloy is even better than the pure $Fe_{90}Sc_{10}$ MNG (1.05 μ_B per Fe atom).[6] The magnetism increases significantly with the initial addition of the ~$Fe_{90}Sc_{10}$ component and then increases slowly (Figure 4(b)). Eventually, it starts to decrease at the compositions above 75 at.%. For a two-component system, it is statistically predicted that a 50:50 distribution of the two nanoglass components could be the transition point as marked in Fig. 4(b). This is almost the crossover point of the two tangent lines T1 and T2, indicating that the 50 at.% addition could be the maximum point of the magnetism. Unfortunately, it is difficult to precisely control the atomic percentage of the ~$Fe_{90}Sc_{10}$ component in the MNG-2 alloys at the present stage. The verification of the existence of such a threshold value will be our next step work. Provided that the magnetism of the pure ~$Fe_{90}Sc_{10}$ MNG is not strongest among the MNG-2 alloys, it is accepted that the introduction of the ~$Cu_{64}Sc_{36}$ component not only reduces the amount of the interfaces among the ~$Fe_{90}Sc_{10}$ nanoglass particles, but also modifies the structure of the ~$Fe_{90}Sc_{10}$ component. Because the magnetic moment of iron is increased with the interatomic spacing of Fe-Fe pairs, [26, 27] the enhanced magnetization is supposed to originate from the enlarged average interatomic spacing of Fe-Fe pairs possibly associated with the repulse from Cu due to the immiscibility of Cu and Fe. The detailed interpretation of the magnetism needs a combination of a thorough magnetic structural analysis and computational simulations,[28] which is already out of the scope of the present study.

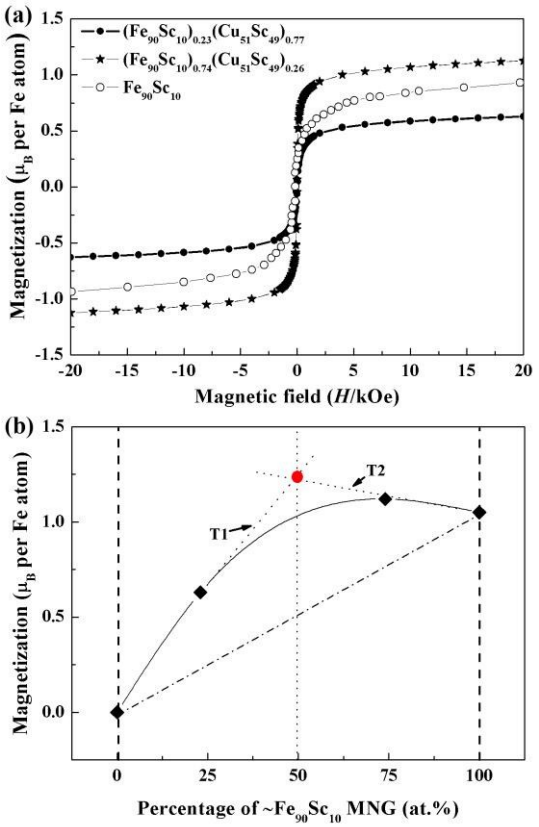

Fig. 4 (a) The *M-H* curves of the MNG-2 alloys and (b) the magnetization variation with different atomic percentages of the $Fe_{90}Sc_{10}$ MNG component in the MNG-2 alloys.

Formation of new materials with unique structures is one of the focused issues in materials science. In particular, interface-induced drastic property changes offer great potentials for achieving new functionalities and unprecedented device concepts.[29, 30] However, resolving the correlation between the interfaces and the properties of a material remains challenge, particularly in the materials with diffused interfaces. Nanoscale phase separation is normally explored to produce a BMG comprising of two MG phases,[22, 31] which is supposed to stabilize the amorphous phase by lowering the enthalpy and the free energy of the mutually immiscible alloy systems.[32, 33] In the case of our present study, the nanoalloying of immiscible Cu and Fe helps quantify the role of interfaces and further build a reliable correlation between the structure and properties. To our best knowledge, this is the first nanoglass alloy system to show tunable properties. In addition, there is usually vast solubility difference in liquid states in comparison to crystalline states for most systems. A popular example is the solubility of sugar or salt in water but not in ice. As glasses have essentially similar structures as frozen liquids, one can expect to produce non-crystalline solid solutions of components that are totally immiscible in their crystalline states. In

other words, nanoglass alloys may open an avenue to an entirely new world of solid solutions and these new solid solutions are likely - due to their novel chemical compositions - to have properties that are yet unknown in today's alloys.

Experimental

The ~10 nm-sized nanoglass particles are produced by the inert gas condensation, from which the bulk metallic nanoglass (MNG) samples are formed in a diameter of 8 mm using in-situ compaction at 1.5 GPa. During the production of nanoglass particles, the evaporation rates of the metals present in the final alloy are different. This may yield compositions of the nanoglasses at the beginning of the synthesis largely different from those at the end of the process. The evaporation rates are mainly determined by the vapor pressure of the evaporated metals, corrected by the respective heats of mixing between the constituents. To avoid large compositional differences, the alloy systems have to be selected based on the parameters including the saturation vapor pressure, the molecular weight and the heats of mixing. In the present study, an alloy combination was selected which is characterized by immiscibility of the two major components, i.e., Fe and Cu. As a result, the binary nanoglass-forming systems, for example, Fe-Sc and Cu-Sc alloys, were selected. Meanwhile, the choice of simple two-component alloys simplifies the control of the synthesis. In addition, we selected the components with close values of the saturation pressure and the molecular weight. For the Fe-Sc system, the evaporation rates of Fe and Sc are almost the same. It has been demonstrated in previous experiments that the nanoglasses can be formed with an average composition of ~$Fe_{90}Sc_{10}$ accompanied by a compositional deviation less than 5 at.% using an ingot with a nominal composition of ~$Fe_{85}Sc_{15}$. For the Cu-Sc system, the evaporation rate of Cu is higher than that of Sc. Taken into account the glass-forming compositions required to be close to their eutectic points, the ingot composition is determined as ~$Cu_{52}Sc_{48}$. Meanwhile, we prepared much larger ingots than the amount for formation of one piece of MNG alloy to reduce the effect of different evaporation rates on the residual ingot compositions. By appropriately controlling the experimental parameters, for example, reducing the heating power and the inert gas flow, the Cu-Sc nanoglass compositional difference could be well controlled within 5 at.% in one piece of sample. The structures of both nanoglass particles and MNG samples are investigated by a combination of high resolution transmission electron microscopy (HRTEM) and aberration-corrected scanning transmission electron microscopy (STEM) methods. The TEM specimens from the MNG samples are prepared by grinding the MNG alloys into powders in an acetone solution. Partial crystallization and oxidation are induced by the mechanical energy transfer during the grinding. Magnetic properties of the bulk MNG samples are measured by using SQUID-VSM of Quantum Design Company.

Conclusions

Using inert gas condensation we have produced different MNG alloys consisting of two nanoglass components of $Cu_{64}Sc_{36}$ and $Fe_{90}Sc_{10}$. The incorporation of the ~$Cu_{64}Sc_{36}$ nanoglass in the MNG alloys reduces the amount of the interfaces between the ~$Fe_{90}Sc_{10}$ nanoparticles, which enables tuning of the magnetic properties. This could be useful for building a reliable structure-property correlation of nanoglasses. Attributed to their controllable properties, the MNG alloys may trigger intensive studies in design concepts of emerging materials with unique structures.

Author Information

Corresponding Author
*E-mail: chennadm@mail.tsinghua.edu.cn

Notes

The authors declare no competing financial interest.

Acknowledgements

Financial support by the Helmholtz Association and the State of Hessen is kindly acknowledged. This work is also sponsored by "World Premier International Research Center (WPI) Initiative for Atoms, Molecules and Materials", the National Natural Science Foundation of China (Grant No. 51471091) and Beijing Municipal Natural Science Foundation (Grant No. 2152015).

Notes and references

[a] Institute for Nanotechnology, Karlsruhe Institute of Technology (KIT), Karlsruhe 76021, Germany.
[b] WPI Advanced Institute for Materials Research (WPI-AIMR), Tohoku University, Sendai 980-8577, Japan.
[c] School of Materials Science and Engineering, Tsinghua University, Beijing 100084, P.R. China.
[d] Nanjing University of Science and Technology, Herbert Gleiter Institute of Nanoscience, Building 340, Nanjing, Jiangsu 2 10094, P. R. China.
[e] Joint Research Laboratory Nanomaterials, Technische Universität Darmstadt, Darmstadt 64287, Germany.

1 H. Gleiter, *Acta Mater.*, 2008, **56**, 5875.
2 N. Chen, R. Frank, N. Asao, D. V. Louzguine-Luzgin, P. Sharma, J. Q. Wang, G. Q. Xie, Y. Ishikawa, N. Hatakeyama, Y. C. Lin, M. Esashi, Y. Yamamoto and A. Inoue, *Acta Mater.*, 2011, **59**, 6433.
3 J. X. Fang, U. Vainio, W. Puff, R. Würschum, X. L. Wang, D. Wang, M. Ghafari, F. Jiang, J. Sun, H. Hahn and H. Gleiter, *Nano Lett.*, 2012, **12**, 458.
4 N. Chen, D. V. Louzguine-Luzgin, G. Q. Xie, P. Sharma, J. H. Perepezko, M. Esashi, A. R. Yavari and A. Inoue, *Nanotechnology*, 2013, **24**, 045610.
5 M. Ghafari, H. Hahn, H. Gleiter, Y. Sakurai, M. Itou and S. Kamali, *Appl. Phys. Lett.*, 2012, **101**, 2431041.
6 R. Witte, T. Feng, J. X. Fang, A. Fischer, M. Ghafari, R. Kruk, R. A. Brand, D. Wang, H. Hahn and H. Gleiter, *Appl. Phys. Lett.*, 2013, **103**, 073106.
7 G. Kumar, H. X. Tang and J. Schroers, *Nature*, 2009, **457**, 868.
8 N. Chen, X. T. Shi, R. Witte, K. Nakayama, K. Ohmura, H. Wu, A. Takeuchi, H. Hahn, M. Esashi, H. Gleiter, A. Inoue and D. V. Louzguine, *J. Mater. Chem. B*, 2013, **1**, 2568.

9 H. Gleiter, T. Schimmel and H. Hahn, *Nano Today*, 2014, **9**, 17.
10 S. Adibi, Z. D. Sha, P. S. Branicio, S. P. Joshi, Z. S. Liu and Y. W. Zhang, *Appl. Phys. Lett.*, 2013, **103**, 211905.
11 I. Singh, R. Narasimhan and Y. W. Zhang, *Philos. Mag. Lett.*, 2014, **94**, 678.
12 D. Sopu, Y. Ritter, H. Gleiter and K. Albe, *Phys. Rev. B*, 2009, **83**, 10202.
13 E. Kneller, *J. Appl. Phys.*, 1962, **33**, 1355.
14 P. A. Flynn, B. L. Averbach and M. Cohen, *Acta Matell.*, 1953, **1**, 664.
15 E. Kneller, *J. Appl. Phys.*, 1964, **35**, 2210.
16 E. Ma, *Prog. Mater. Sci.*, 2005, **50**, 413.
17 R. K. Linde, *J. Appl. Phys.*, 1966, **37**, 934.
18 V. Petkov, B. N. Wanjala, R. Loukrakpam, J. Luo, L. Yang, C. Zhong and S. Shastri, *Nano lett.*, 2012, **12**, 4289.
19 A. E. Berkowitz, J. R. Mitchell, M. J. Carey, A. P. Young, S. Zhang, F. E. Spada, F. T. Parker, A. Hutten and G. Thomas, *Phys. Rev. Lett.*, 1992, **68**, 3745.
20 J. Das, M. B. Tang, K. B. Kim, R. Theissmann, F. Baier, W. H. Wang and J. Eckert, *Phys. Rev. Lett.*, 2005, **94**, 205501.
21 K. F. Yao, F. Ruan, Y. Q. Yang and N. Chen, *Appl. Phys. Lett.*, 2006, **88**, 122106.
22 D. H. Kim, W. T. Kim, E. S. Park, N. Mattern and J. Eckert, *Prog. Mater. Sci.*, 2013, **58**, 110.
23 R. Tauler, A. Smilde and B. Kowalski, *J. Chemometr.*, 1995, **9,** 31.
24 A. de Juan and R. Tauler, *Anal. Chim. Acta*, 2003, **500**, 195.
25 M. Ghafari, S. Kohara, H. Hahn, H. Gleiter, T. Feng, R. Witte and S. Kamali, *Appl. Phys. Lett.*, 2012, **100**, 133111.
26 C. A. F. Vaz, J. A. C. Bland and G. Lauhoff, *Rep. Prog. Phys.*, 2008, **71**, 056501.
27 L. Del Bianco, C. Ballesteros, J. M. Rojo and A. Hernando, *Phys. Rev. Lett.*, 1998, **81**, 4500.
28 A. stoesser, M. Ghafari, A. Kilmametov, H. Gleiter, Y. Sakurai, M. Itou, S. Kohara, H. Hahn and S. Kamali, *J. Appl. Phys.*, 2014, **116**, 134305.
29 H. Y. Hwang, Y. Iwasa, M. Kawasaki, B. Keimer, N. Nagaosa and Y. Tokura, *Nat. Mater.*, 2012, **11**, 103.
30 J. Mannhart and D. G. Schlom, *Science*, 2010, **327**, 1607.
31 B. J. Park, H. J. Chang, D. H. Kim, W. T. Kim, K. Chatoadhyay, T. A. Abinandanan and S. Bhattacharyya, *Phys. Rev. Lett.*, 2006, **96**, 245503.
32 J. H. He, H. W. Shen, P. J. Schilling, C. -L. Chien and E. Ma, *Phys. Rev. Lett.*, 2001, **86**, 2826.
33 R. Banerjee, A. Puthucode, S. Bose and P. Ayyub, *Appl. Phys. Lett.*, 2007, **90**, 021904.